Rok Cestnik | Michael Rosenblum

Reconstructing networks of pulse-coupled oscillators from spike trains

Suggested citation referring to the original publication:
Physical review E 96 (2017), Art. 012209
DOI https://doi.org/10.1103/PhysRevE.96.012209
ISSN (print) 2470-0045
ISSN (online) 2470-0053

Reconstructing networks of pulse-coupled oscillators from spike trains

Rok Cestnik[1,2,*] and Michael Rosenblum[1,3,†]

[1]*Department of Physics and Astronomy, University of Potsdam, Karl-Liebknecht-Strasse 24/25, D-14476 Potsdam-Golm, Germany*

[2]*Department of Human Movement Sciences, MOVE Research Institute Amsterdam, Vrije Universiteit Amsterdam, van der Boechorststraat 9, Amsterdam, Netherlands*

[3]*The Research Institute of Supercomputing, Lobachevsky National Research State University of Nizhny Novgorod, Russia*

(Received 23 March 2017; published 12 July 2017)

We present an approach for reconstructing networks of pulse-coupled neuronlike oscillators from passive observation of pulse trains of all nodes. It is assumed that units are described by their phase response curves and that their phases are instantaneously reset by incoming pulses. Using an iterative procedure, we recover the properties of all nodes, namely their phase response curves and natural frequencies, as well as strengths of all directed connections.

DOI: 10.1103/PhysRevE.96.012209

I. INTRODUCTION

Reconstruction of a network structure from observations is an important problem relevant for many different areas such as neuroscience [1], physiology [2], climatology [3], genetics [4], ecology [5], etc. A group of established reconstruction techniques relies on analysis of the system's response to a specially designed perturbation, i.e., on invasive measurements [6]. However, often invasive measurement is not an option, e.g., in problems related to climatology, physiological studies, and medical diagnostics. In such cases one is restricted to analysis of observations of the free-running system.

Roughly speaking, there are two approaches to the problem. The first one does not imply any assumptions about the dynamics of the nodes and properties of the links and relies on different statistical and information-theoretical techniques for quantification of all connections [7]. In the second, model-based approach, some properties of the nodes (e.g., existence of a stable limit cycle) and of the links (e.g., weakness of coupling) are assumed to be known [8–11]. In the present work, we follow and extend the model-based approach. The main assumption is that the networks can be modeled by coupled limit cycle oscillators [12,13]. In this way, we follow our previous studies, where we have reconstructed the connectivity of a weakly coupled network of noisy limit-cycle or weakly chaotic oscillators for the case when the measurements allow for the determination of instantaneous phases [10,14]; see also Refs. [15,16].

In this paper, we address the case when the signals are spiky, namely, that the measurements between the spiking events are dominated by noise and only determination of the times of spikes is reliable. Hence, the data we analyze are spike trains and estimation of time-continuous phase is not feasible. Next, we assume that effect of a chosen unit on the rest of the network is restricted to the time instant when the unit generates a spike. Thus, we use the model of pulse-coupled neuronlike oscillators [17,18]. Assuming that the outputs of all nodes are known, that there are no unobserved external inputs, and that the coupling between the elements is sufficiently weak to justify the phase dynamics description, we recover the connectivity of the network and properties of all its nodes.

The paper is organized as follows. In Sec. II, we describe in details the model and summarize all the assumptions. In Sec. III, we introduce our technique and in Sec. IV, we present the results of numerical studies. Section V presents discussion of the results.

II. THE MODEL

Our basic model for the network's node is a limit cycle oscillator that issues a spike when its phase φ achieves 2π. (We consider the phases wrapped to the $[0,2\pi)$ interval, i.e., after the spike generation the phase of the unit is reset to zero.) This spike affects all other units of the network according to the strength of the corresponding outcoming connections. Let the size of the network be N and let the connectivity be described by an $N \times N$ coupling matrix $\mathcal{E}$, whose elements ε_{ij} quantify the strength of the coupling from unit j to unit i. Between the spiking events, phases of all units obey $\dot{\varphi}_i = \omega_i$, where ω_i are frequencies. If unit i receives a spike from oscillator j, then it reacts to the stimulus according to its so-called phase response curve (PRC), $Z_i(\varphi)$ [19,20]. This means that the phase of the stimulated unit is instantaneously reset, $\varphi_i \to \varphi_i + \varepsilon_{ij} Z_i(\varphi_i)$.

Notice that oscillators are generally nonidentical: they have different frequencies and different PRCs. However, we assume that response of the unit i to the stimuli from different units is described by the same PRC Z_i. Furthermore, we assume that PRCs are continuous. Next, the coupling is taken to be bidirectional but generally asymmetric, i.e., $\varepsilon_{ji} \neq \varepsilon_{ij}$, and there is no self-action, i.e., $\varepsilon_{ii} = 0$. Finally, we assume that there is no delay in coupling, i.e., that time of pulse propagation is much smaller than minimal interspike interval and can be neglected.

In neuronal modeling one commonly identifies two types of PRCs: if spikes always shorten the period of the stimulated unit, then the PRC is classified as type I; otherwise, if depending on the phase of the stimulation, the period can be either shortened or prolonged, then the PRC is classified as type II [20,21]. We model the type I PRC as

$$Z(\varphi) = [1 - \cos(\varphi)] \exp\{3[\cos(\varphi - \varphi_0) - 1]\}, \qquad (1)$$

*rokcestn@uni-potsdam.de

†mros@uni-potsdam.de

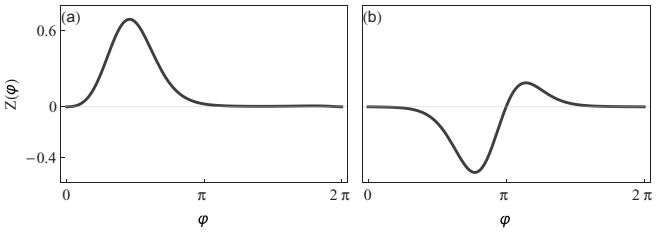

FIG. 1. Model phase response curves of type I (a) and type II (b).

and the type II PRC as

$$Z(\varphi) = -\sin(\varphi)\exp\{3[\cos(\varphi-\varphi_0)-1]\}, \qquad (2)$$

where the parameter values are $\varphi_0 = \pi/3$ and $\varphi_0 = 0.9\pi$, respectively. The plots of these curves are shown in Fig. 1.

Simulating this model, we generate N point processes (spike trains) and then use them for network reconstruction, where we estimate the coupling matrix $\mathcal{E}$, PRCs $Z_i(\varphi)$, and frequencies ω_i of all elements, as discussed in the next section. There we also present the results of a test with a more realistic model of coupled Morris-Lecar neuronal oscillators [22].

III. THE TECHNIQUE

For each node we reconstruct its properties as well as strength of all incoming connections. For definiteness, we always determine these quantities for the first node; the procedure then shall be repeated for all other units. Thus, we recover ε_{1j}, Z_1, and ω_1; for simplicity of presentation, in the following we omit the subscript 1.

We solve the reconstruction problem by iterations. First, since we do not have any *a priori* knowledge of the system, we assign some values to the coupling coefficients (we discuss several options of how this can be done) and use them in order to obtain a first estimate of the PRC. The knowledge of the latter allows for an improved estimation of the network connectivity, which is then in turn used to obtain a better approximation of the PRC, and so on. We demonstrate that the procedure converges quite fast.

A. Notations and phase equations

Let the pulse train of the first oscillator contain $M+1$ spikes at times $t_k^{(1)}$, so that we have M interspike intervals $T_k = t_{k+1}^{(1)} - t_k^{(1)}$. In the following, we treat each interval separately. Suppose that within the interspike interval T_k the first unit receives n stimuli from the unit i, we denote this number as $n_k(i)$. These stimuli appear at instants of time $t_k^{(i,l)}$, $l = 1,\ldots,n_k(i)$. The times relative to the beginning of the interval are denoted as $\tau_k^{(i,l)} = t_k^{(i,l)} - t_k^{(1)}$; see Fig. 2 for illustration. Respective phases of the first unit are denoted as $\varphi(t_k^{(1)} + \tau_k^{(i,l)}) = \varphi_k^{(i,l)}$.

The phase increase within each interspike interval is

$$\omega T_k + \sum_{i=2}^{N}\varepsilon_i \sum_{l=1}^{n_k(i)} Z\left(\varphi_k^{(i,l)}\right) = 2\pi, \qquad (3)$$

where the first term reflects the autonomous dynamics, whereas the second term describes the effect of pulse coupling.

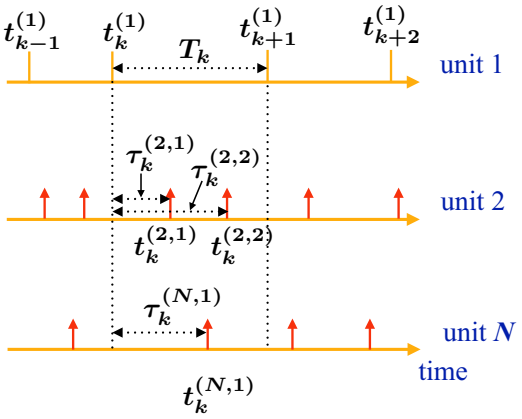

FIG. 2. Illustration of notations used. T_k is an interspike interval of the driven unit. $\tau_k^{(i,l)}$ is the time (relative to the beginning of the interval T_k) when the spike number l from the unit number i arrives.

M interspike intervals yield a system of M Eqs. (3) for unknown coupling coefficients ε_i, frequency ω, and the PRC Z of the driven unit.

Assume for the moment that the coupling coefficients ε_i are given. Then, representing the unknown $Z(\varphi)$ as a finite Fourier series of order N_F, we obtain from Eqs. (3) a system of linear equations for $2N_F+1$ Fourier coefficients and the unknown frequency ω. For a long time series, $M > 2N_F+2$, this is an overdetermined system which can be solved, e.g., by a least-mean-square fit or by singular value decomposition; see Ref. [23]. On the other hand, if PRC is given, we again obtain a solvable linear system for $N-1$ coupling coefficients ε_i and frequency ω [24]. Thus, having an initial estimate for either PRC or coupling coefficients (practically we use the latter option) we can try to solve Eqs. (3) by iterations.

B. First iteration

The phases within each interspike interval vary from zero to 2π. For the first iteration we take the simplest approximation, i.e., we compute the phases as growing proportionally to time. Hence, when a spike at $\tau_k^{(i,l)}$ arrives, the phase of the first unit is taken as

$$\varphi_k^{(i,l)} \approx 2\pi\,\tau_k^{(i,l)}/T_k. \qquad (4)$$

Since in this approximation we neglect the phase resets, $\varphi \to \varphi + \varepsilon_i Z(\varphi)$, the errors of such a phase estimation are of the order of $\varepsilon_i\|Z\|$, where $\|\cdot\|$ is the norm of the function, and accumulate with the number of the incoming spikes.

Next, we have to choose some initial values for the coupling coefficients ε_i. There are several options on how to do this. First, we can exploit the simple idea that if there is no connection to the first unit from the unit i, then T_k cannot depend on the phase when the spikes from this unit appear, i.e., there shall be no dependence of T_k on $\varphi_k^{(i,1)}$. On the other hand, if this connection exists, the dependence of T_k on $\varphi_k^{(i,1)}$ shall be present as well; moreover, the larger ε_i, the stronger this dependence shall be. As shown in the Appendix, this idea indeed works well for long time series. Alternatively, we can assign the same value to all ε_i, or we can take them randomly.

C. Next iterations

In the first approximation, we compute the phases proportionally to time; see Eq. (4). If the coupling strength, ε_i, and parameters of the system, i.e., ω and Z, are already estimated, then we can use this knowledge for a more precise estimation of the phases. For illustration, suppose that within the interspike interval T_k the first unit receives three stimuli at times $\tau_k^{(i,1)} < \tau_k^{(m,1)} < \tau_k^{(n,1)}$. Then the phases at these three instances are computed as

$$\begin{aligned}
\varphi_k^{(i,1)} &= \omega\tau_k^{(i,1)},\\
\varphi_k^{(m,1)} &= \omega\tau_k^{(m,1)} + \varepsilon_i Z\big(\varphi_k^{(i,1)}\big),\\
\varphi_k^{(n,1)} &= \omega\tau_k^{(n,1)} + \varepsilon_i Z\big(\varphi_k^{(i,1)}\big) + \varepsilon_m Z\big(\varphi_k^{(m,1)}\big).
\end{aligned}$$

The phase at the end of the given interspike interval is

$$\psi = \omega T_k + \varepsilon_i Z\big(\varphi_k^{(i,1)}\big) + \varepsilon_m Z\big(\varphi_k^{(m,1)}\big) + \varepsilon_n Z\big(\varphi_k^{(n,1)}\big). \quad (5)$$

By definition, this value should be equal to 2π. However, since ω, Z and coupling coefficients ϵ_i are not exact, ψ generally differs from 2π. Therefore, we rescale all phase estimates by the factor $2\pi/\psi$.

Now, using the newly estimated phases and the estimation of the PRC from the previous iteration, we can compute new values of the coupling coefficients ε_i, and then repeat the whole procedure. As we demonstrate below, these iterations converge quite quickly.

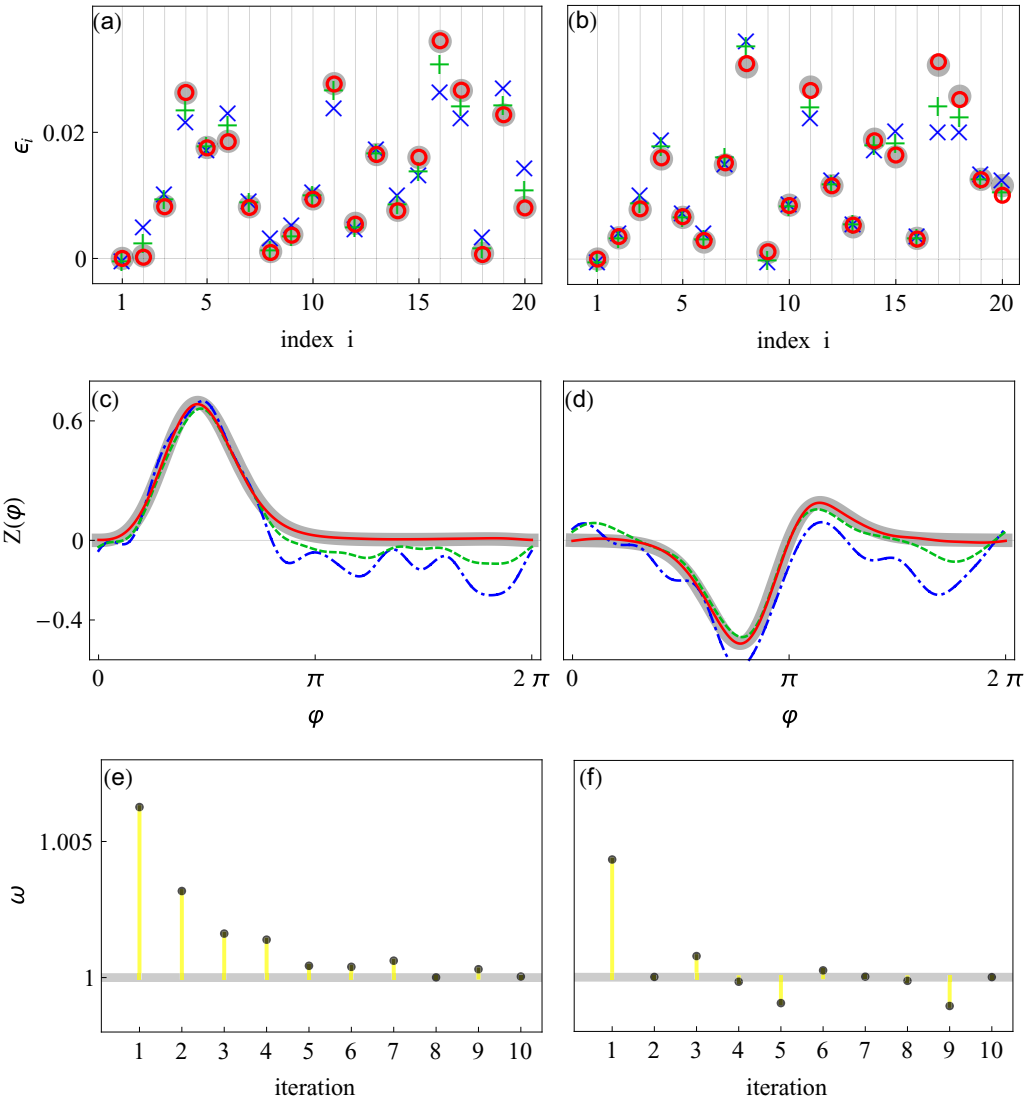

FIG. 3. Reconstruction of a network of 20 units using $M = 200$ interspike intervals. Panels (a, c, e) and (b, d, f) show the results for PRC type I and PRC type II, respectively; see Eqs. (1) and (2). (a, b) Strength of incoming connections for the first oscillator: true values (gray disks) and values recovered after 1, 2, and 10 iterations (blue crosses, green pluses, and red circles, respectively). (c, d) True (wide gray curve) and reconstructed PRCs, after 1, 2, and 10 iterations (blue dashed-dotted, green dashed, and red solid curves, respectively). (e, f) Estimated natural frequencies as functions of the iteration number; the true value $\omega = 1$ is shown by horizontal gray line. Notice that in this figure we illustrate the most difficult case of the slowest node.

IV. NUMERICAL TESTS

In this section, we present the results of numerical testing of our reconstruction algorithm. For this goal we generate the networks with some randomly chosen parameters and simulate them to obtain the data. Next, we recover the networks from these data and compare the reconstructed parameter values with the true ones.

A. Basic model

In this test, for acceleration of data generation we assign identical PRCs to all nodes; however, because each node of the network is treated separately, this feature is neither used for reconstruction nor implies any limitations in the applicability of the algorithm. First, we consider networks of $N = 20$ oscillators, with natural frequencies taken from a uniform distribution between 1 and 2. Strength of network links is sampled from the positive half of a Gaussian distribution with zero mean and standard deviation 0.02. The frequency of the first oscillator is set to 1, assuring that it is the slowest one (as discussed below, this is the most difficult case) and then we reconstruct its PRC Z, frequency ω, and strength of all incoming links ε_i, $i = 2, \ldots, 20$. We exclude from the consideration the networks where at least two units synchronized. We use ten iterations of the procedure described above. The number of the Fourier harmonics approximating the PRC is $N_F = 10$, which is sufficient to describe PRCs of common neuronal models.

Before presenting the results we recall that all equations contain ε_i and Z in products of each other. Therefore, solutions $\{\varepsilon_i, Z\}$ and $\{c\varepsilon_i, Z/c\}$, where c is an arbitrary constant, are equivalent. The factor c has no physical meaning by itself, but since we want to compare the reconstructed values with the originally given, we have to fix it. Quite arbitrarily, we do it

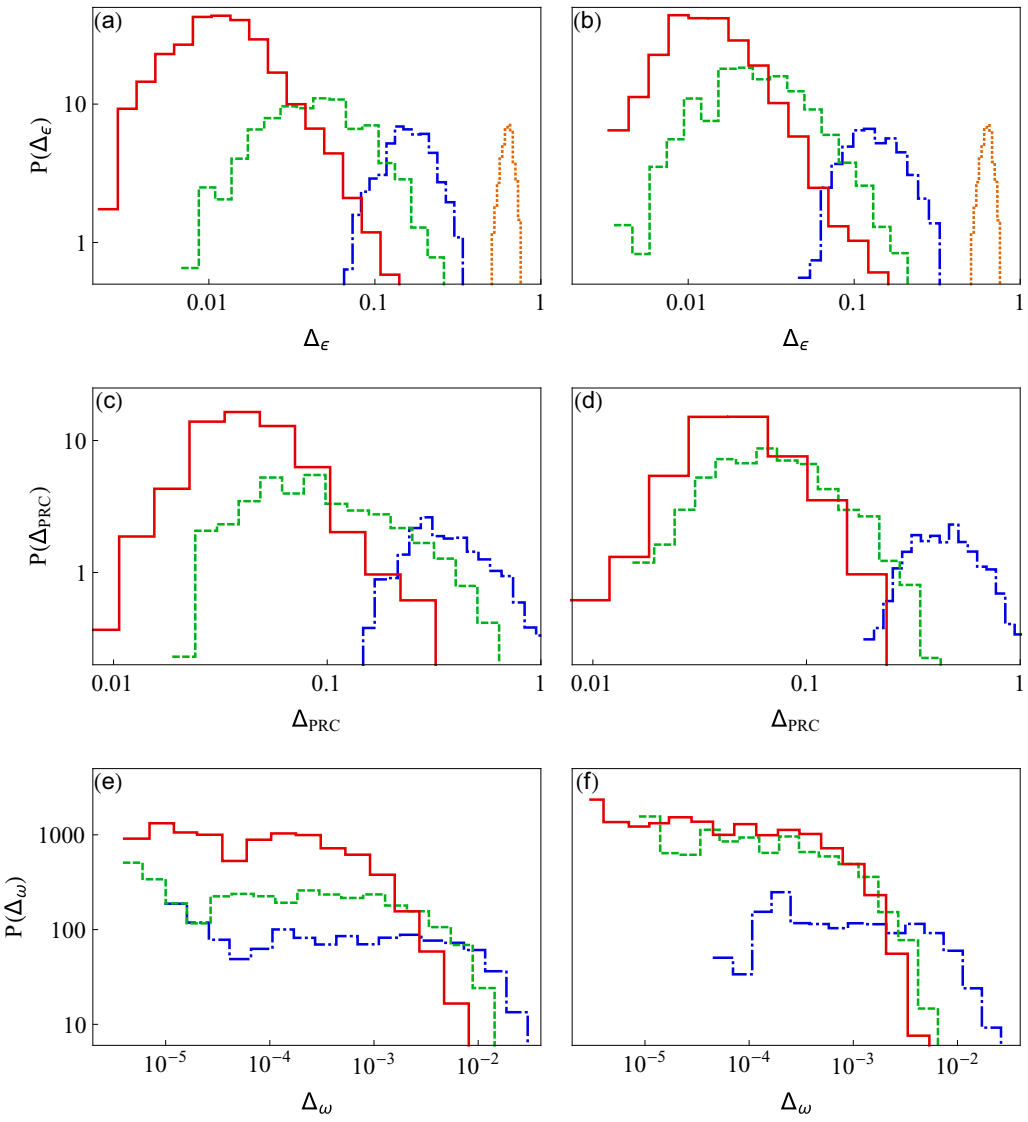

FIG. 4. Histograms of errors of the coupling strengths Δ_ε (a, b), PRC Δ_{PRC} (c, d), and frequency $\Delta\omega$ (e, f); see Eqs. (7)–(9). Panels (a, c, e) and (b, d, f) correspond to tests with PRC type I and type II, respectively. In each panel, the results of the first, third, and tenth iterations are shown in blue (dash-dotted), green (dashed), and red (solid line), respectively. In (a, b) also the distribution of errors for initial values $\varepsilon_i = 1$ is shown in orange (dotted line).

by minimizing

$$\sum_{i=2}^{N}\left[\varepsilon_i^{(\mathrm{t})} - c\varepsilon_i^{(\mathrm{r})}\right]^2,$$

where the superscripts (t) and (r) stand for true and reconstructed, respectively. This condition yields

$$c = \sum_{i=2}^{N}\varepsilon_i^{(\mathrm{t})}\varepsilon_i^{(\mathrm{r})} \Big/ \sum_{i=2}^{N}\left[\varepsilon_i^{(\mathrm{t})}\right]^2. \tag{6}$$

Using this normalization, we show the results of a particular run in Fig. 3; for this computation we took initially $\varepsilon_i = 1$, $\forall i$.

Next, we perform a statistical analysis for 10^5 network configurations. To quantify the quality of the reconstruction, we define the corresponding errors for recovered PRC, ε_i, and ω as

$$\Delta^2_{\mathrm{PRC}} = \frac{\int_0^{2\pi}[Z^{(\mathrm{t})}(\varphi) - Z^{(\mathrm{r})}(\varphi)]^2 d\varphi}{\int_0^{2\pi}[Z^{(\mathrm{t})}(\varphi)]^2 d\varphi}, \tag{7}$$

$$\Delta^2_{\varepsilon} = \sum_{i=2}^{N}\left[\varepsilon_i^{(\mathrm{t})} - \varepsilon_i^{(\mathrm{r})}\right]^2 \Big/ \sum_{i=2}^{N}\left[\varepsilon_i^{(\mathrm{t})}\right]^2, \tag{8}$$

and

$$\Delta^2_{\omega} = [\omega^{(\mathrm{t})} - \omega^{(\mathrm{r})}]^2, \tag{9}$$

respectively [25]. The distributions of errors, shown in Fig. 4, confirm robustness of the iterative procedure. Figure 5 shows the dependence of the reconstruction error on the number of interspike intervals. Naturally, the more data we use, the better results we expect. This test demonstrates, that reasonable reconstruction can be achieved already for several hundreds of intervals.

Additionally, instead of initially assigning the same value to all coupling coeffiecient ε_i, we also performed the test with random assignment of the initial values. For several generated

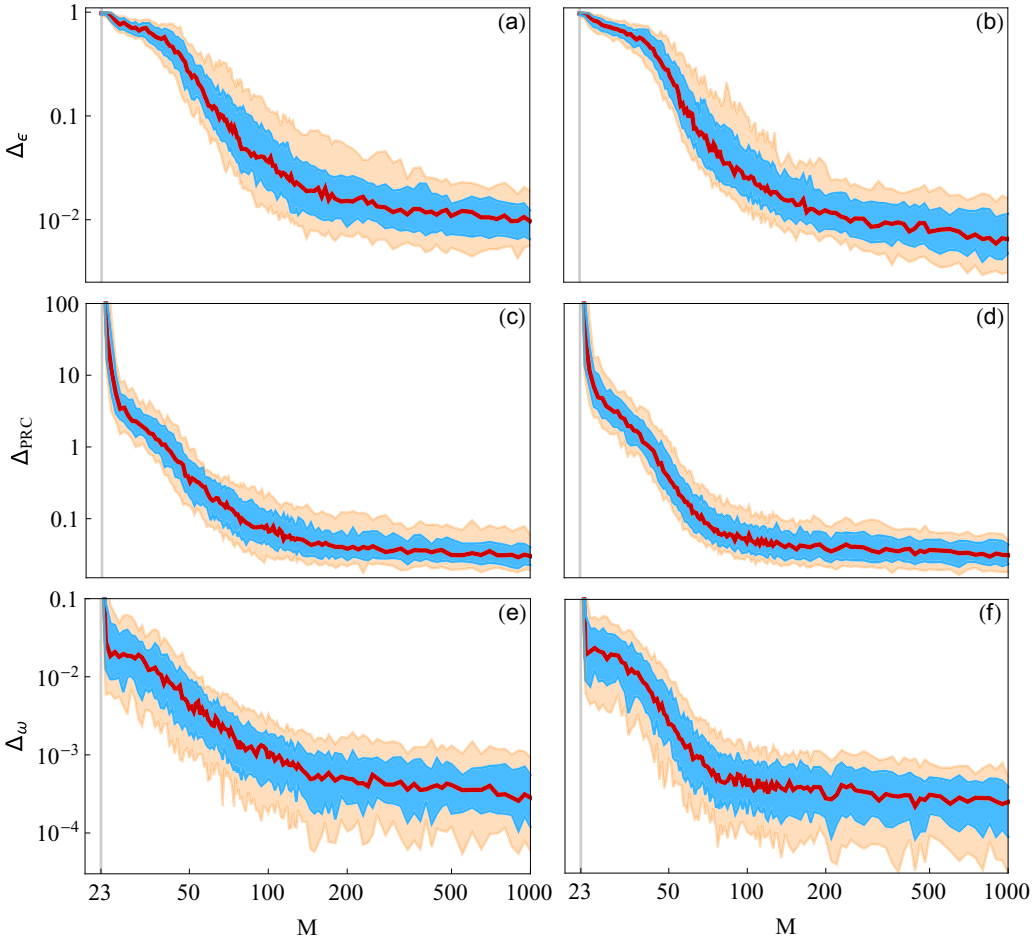

FIG. 5. Error of the reconstruction in dependence on the number of interspike intervals M used for the analysis. Panels (a, c, e) and (b, d, f) show the results for PRC type I and PRC type II, respectively. Panels (a, b) show the error of the coupling coefficients ε_i Eq. (7), panels (c, d) the error of the PRC Eq. (8) and panels (e, f) the error of the frequency ω Eq. (9). For each value of M reconstruction error was computed for 6000 different networks. The blue (dark gray) and the orange (light gray) areas contain 50% and 75% of the errors, respectively; the median is shown in red (bold line).

networks we performed 10^4 reconstructions with different initial ε_i. The results confirm convergence of the algorithm for this case as well.

To conclude the presentation of the algorithm, we briefly discuss its stability with respect to noise as well as its computational complexity. We have tested our method on data generated with dynamical white noise, $\dot{\varphi}_i = \omega_i + \xi_i$, and found that for weak noise, the errors of the reconstruction scale roughly linearly with the standard deviation of the noise, σ_ξ, i.e., $\Delta_X = \kappa_X \sigma_\xi$, where scaling coefficients are $\kappa_\varepsilon \approx 40$, $\kappa_{\mathrm{PRC}} \approx 100$, and $\kappa_\omega \approx 1$. Regarding the computational complexity of the algorithm, we note that, at each iteration, recovering incoming connections of one node requires least-squares minimization of an $M \times N$ system (for ε_i) and $M \times (2N_F + 2)$ system (for PRC). Assuming that N_F can be kept constant, we arrive at $O(N^3 M)$ asymptotic scaling dependence for reconstruction of the whole network. Since the number of intervals M should always be greater than the number of oscillators N in order to have an over-determined system, we took $M \propto N$ and measured the computation time for different system sizes ranging from $N = 10$ to $N = 500$. Within that range the error of the reconstruction was roughly constant and the computation time scaled like $O(N^4)$, as expected. In fact, computations are very fast: for $M = 1000$ interspike intervals, a single iteration of the reconstruction of one node's incoming connections in a network of 100 oscillators takes about 1 s on a common desktop computer.

B. Network of Morris-Lecar neurons

In the next test we make a step toward more realistic modeling and consider a network of Morris-Lecar neurons [22]. The equations of the network are

$$\begin{aligned} \dot{V}_i &= I_i - g_L(V_i - V_L) - g_K w_i (V_i - V_K) \\ &\quad - g_{Ca} m_\infty(V_i)(V_{Ca} - V_i) + I_i^{(\mathrm{syn})}, \\ \dot{w}_i &= \lambda(V_i)(w_\infty(V_i) - w_i), \end{aligned} \tag{10}$$

where

$$\begin{aligned} m_\infty(V) &= [1 + \tanh(V - V_1/V_2)]/2, \\ w_\infty(V) &= [1 + \tanh(V - V_3/V_4)]/2, \\ \lambda(V) &= \cosh[(V - V_3)/(2V_4)]/3, \end{aligned} \tag{11}$$

and $I_i^{(\mathrm{syn})}$ is the total incoming synaptic current. We write the latter as

$$I_i^{(\mathrm{syn})} = [V_{\mathrm{rev}} - V_i] \sum_{j, j \neq i} \frac{\varepsilon_{ij}}{1 + \exp[-(V_j - V_{\mathrm{th}})/\sigma]}. \tag{12}$$

We take standard values for most of the parameters [26]. Parameters of the synaptic coupling are $V_{\mathrm{rev}} = 0.2$, $V_{\mathrm{th}} = 0.25$, and $\sigma = 0.01$. The neurons are nonidentical: the values of the current are $I_i = 0.077[1 + 0.22\ \mathcal{U}(0,1)]$, where $\mathcal{U}(0,1)$ is a uniformly distributed random number between zero and one; for these values the neurons remain in the spiking state. Similarly to the previous test, we assure that the first oscillator is the slowest by setting its current to the minimal value, $I_1 = 0.077$. The results of the analysis for 20 neurons and 200 interspike intervals, shown in Fig. 6, confirm the efficiency of our technique.

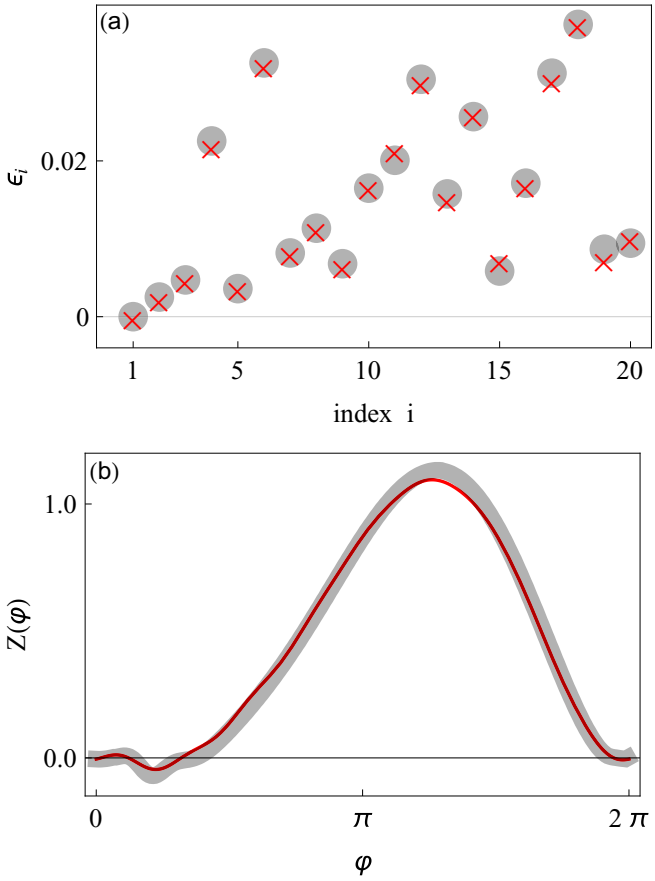

FIG. 6. Reconstruction of a network of 20 Morris-Lecar neuronal oscillators; see Eqs. (10)–(12). 200 interspike intervals were used for the reconstruction. (a) True values of the strength of the incoming connections for the first neuron (gray disks) and these values reconstructed after 10 iterations (red crosses). (b) True (wide gray curve) and reconstructed (solid red curve) PRC. Notice that in this figure we illustrate the most difficult case of the slowest node.

V. DISCUSSION AND CONCLUSIONS

With the help of two model systems we have demonstrated, that our technique provides a robust reconstruction of a network. The data requirements are not too demanding: the reconstruction is quite precise already for time series of several hundreds of spikes. Now we discuss some limitations of the method.

Our approach is based on modeling phase dynamics of a network from data, which assumes weak coupling approximation. If the coupling is not weak enough, the description in terms of PRCs can still be reasonable, but in this case the phase response can be also amplitude-dependent. This means that estimation of the network connectivity remains correct, but the obtained PRC has a limited applicability. Unfortunately, the assumption of weak coupling can be hardly verified from data analysis only. However, we can check the quality of our phase dynamics modeling by looking at the deviation of the phase ψ, see Eq. (5), from 2π. Furthermore, we suggest to perform the reconstruction of the same network many times, starting from different initial values of the coupling strength ε_i and looking for the convergence of the results: if different

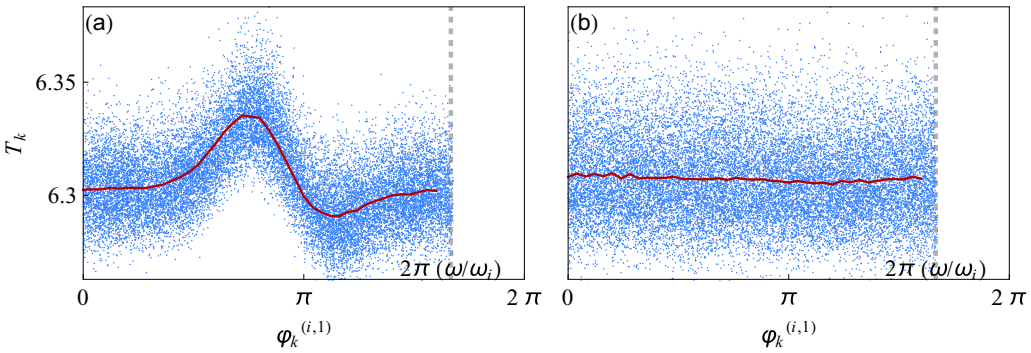

FIG. 7. Scatter plots of interspike intervals T_k vs. approximated phase $\varphi_k^{(i,1)}$ of the first spike from a chosen driving oscillator i, for a strong coupling strength (a) and for a weak one (b). The horizontal axis is divided into $N_b = 50$ bins and solid red curve shows the average of T_k over each of the bins, $\bar{T}^{(i)}$, as a function of the central phase $\bar{\varphi}$ of the bins; 2×10^4 interspike intervals are used in this computation.

initial values yield close network parameters, then the results can be trusted.

Now we comment on the initial estimate of phases using Eq. (4). As already mentioned, the error is proportional to $\varepsilon_i \|Z\|$ and increases with the number of spikes that arrive within the interspike interval of the driven unit. This explains why the case of the slowest oscillator is the most difficult one: such an oscillator has on average more incoming stimuli per interspike interval then the fast units. This means that although our examples demonstrate robust reconstruction, it may fail if $\omega_i/\omega_1 \gg 1$.

Next limitation is related to variability of the interspike intervals of the driving unit i (for $\omega_i > \omega_1$). Indeed, suppose that drive is strictly periodic. Then time of the appearance of the first spike unambiguously determines the timing of the following ones, and hence, the length of the interspike interval T_k. However, T_k is then determined by the sum of different pieces of PRC and this sum cannot be disentangled. The initial estimation of the strength of the connection as described in the Appendix can still work, but the recovery of the PRC becomes impossible and the iterative procedure fails. So, we foresee that reconstruction may be not so robust for very sparse networks where we expect to have purely periodic nodes. On the other hand, a realistic network is noisy, and noise naturally provides the desired variability in the time series, thus enhancing the reconstruction. Finally, we mention that the reconstruction fails if the network synchronizes.

ACKNOWLEDGMENTS

We acknowledge useful discussions with A. Pikovsky, M. Zochowski, R. Andrzejak, and A. Daffertshofer. This work has been financially supported by the European Union's Horizon 2020 research and innovation programme under the Marie Sklodowska-Curie Grant Agreement No. 642563 (COSMOS). Numerical calculations of M. Rosenblum were supported by the Russian Science Foundation Grant No. 17-12-01534.

APPENDIX: FIRST ESTIMATION OF INCOMING CONNECTIONS

For sufficiently long data an initial estimation of the coupling strength ε_i can be performed by evaluating the effect of the first pulse from unit i, that arrives within the kth interspike interval, on the length of this interval T_k. For this purpose, we first plot T_k versus $\varphi_k^{(i,1)}$, for all incoming links. Next, for each plot, we divide the φ-axis into N_b bins and average the T_k values within each bin. As a result, we obtain a dependence $\bar{T}_n^{(i)}(\bar{\varphi}_n)$, where $\bar{\varphi}_n = \frac{\pi}{N_b}(2n-1)$, $n = 1, \ldots, N_b$, are phases at the centers of bins. Our conjecture is that $\bar{T}_n^{(i)}(\bar{\varphi}_n)$ reflects the strength of the incoming connection: if this strength is zero, i.e., there is no incoming link from unit i, then there shall be no dependence; on the other hand, if the incoming connection is strong, then we expect the dependence to be well-pronounced.

We illustrate this idea in Fig. 7, where two such plots are shown for the cases of strong and weak incoming connections. We see that indeed $\bar{T}_n^{(i)}(\bar{\varphi}_n)$ reflects the coupling coefficients ε_i. Hence, we use the standard deviation of this dependence as the first estimate, i.e., we take

$$\varepsilon_i = \left\langle \left(\bar{T}_n^{(i)} - \left\langle \bar{T}_n^{(i)} \right\rangle\right)^2 \right\rangle^{1/2}, \tag{A1}$$

where $\langle\cdot\rangle$ means averaging over N_b bins. Although the correspondence between the estimate and true coupling strength is not exact, in most cases this approach yields reasonable values.

[1] O. Sporns, G. Tononi, and R. Kötter, Comput. Biol. **1**, 245 (2005); J. Riera *et al.*, Phil. Trans. R. Soc. B **360**, 1025 (2005); C. F. Beckmann *et al.*, *ibid.* **360**, 1001 (2005); E. Bullmore and O. Sporns, Nature Rev. Neurosci. **10**, 187 (2009); M. Rubinov and O. Sporns, NeuroImage **52**, 1059 (2010); K. J. Friston, Brain Connect. **1**, 13 (2011); D. Chicharro, R. Andrzejak, and A. Ledberg, BMC Neurosci. **12**, P192 (2011); K. Lehnertz, Physiol. Meas. **32**, 1715 (2011); M. Boly, M. Massimini, M. Garrido, O. Gosseries, Q. Noirhomme, S. Laureys, and A. Soddu, Brain Connect. **2**, 1 (2012); O. Sporns, Nature Methods **10**, 491 (2013).

[2] R. Mrowka, L. Cimponeriu, A. Patzak, and M. Rosenblum, Am. J. Physiol. Regul. Comp. Integr. Physiol. **285**, R1395 (2003); B. Musizza, A. Stefanovska, P. V. E. McClintock, M.

Paluš, J. Petrovčič, S. Ribarič, and F. Bajrovič, J. Physiol. **580**, 315 (2007); B. Kralemann, M. Frühwirth, A. Pikovsky, M. Rosenblum, T. Kenner, J. Schaefer, and M. Moser, Nature Commun. **4**, 2418 (2013).

[3] G. Wang, P. Yang, X. Zhou, K. L. Swanson, and A. A. Tsonis, Geophys. Res. Lett. **39**, L13704 (2012); S. Das Sharma, D. S. Ramesh, C. Bapanayya, and P. A. Raju, J. Geophys. Res. **117**, D13110 (2012).

[4] T. S. Gardner *et al.*, Science **301**, 102 (2003); W. Zhaoa, E. Serpedin, and E. R. Dougherty, Trans. Comput. Biol. Bioinfo. **5**, 262 (2008).

[5] E. L. Berlow *et al.*, J. Animal Ecol. **73**, 585 (2004); M. C. Emmerson and D. Raffaelli, *ibid.* **73**, 399 (2004); G. Sugihara, R. May, H. Ye, C.-h. Hsieh, E. Deyle, M. Fogarty, and S. Munch, Science **338**, 496 (2012); C. Graya, D. H. Figueroa, L. N. Hudson, A. Ma, D. Perkins, and G. Woodward, Food Webs **5**, 11 (2015).

[6] M. Timme, Phys. Rev. Lett. **98**, 224101 (2007); D. Yu and U. Parlitz, Europhys. Lett. **81**, 48007 (2008); PLoS ONE **6**, e24333 (2011); Z. Levnajić and A. Pikovsky, Phys. Rev. Lett. **107**, 034101 (2011).

[7] A. Aertsen and G. L. Gerstein, Brain Res. **340**, 341 (1985); T. Schreiber, Phys. Rev. Lett. **85**, 461 (2000); M. Paluŝ and A. Stefanovska, Phys. Rev. E **67**, 055201 (2003); S. Frenzel and B. Pompe, Phys. Rev. Lett. **99**, 204101 (2007); M. Staniek and K. Lehnertz, *ibid.* **100**, 158101 (2008); L. Barnett, A. B. Barrett, and A. K. Seth, *ibid.* **103**, 238701 (2009); D. Chicharro and R. G. Andrzejak, Phys. Rev. E **80**, 026217 (2009); R. G. Andrzejak, D. Chicharro, K. Lehnertz, and F. Mormann, *ibid.* **83**, 046203 (2011); L. Faes, G. Nollo, and A. Porta, *ibid.* **83**, 051112 (2011). J. Runge, J. Heitzig, V. Petoukhov, and J. Kurths, Phys. Rev. Lett. **108**, 258701 (2012); Y. Mishchencko and J. T. Vogelstein, Ann. Appl. Stat. **5**, 1229 (2011); D. Battaglia, A. Witt, F. Wolf, and T. Geisel, PLoS Comput. Biol. **8**, e1002438 (2012); D. Kugiumtzis, Phys. Rev. E **87**, 062918 (2013); G. Tirabassi *et al.*, Sci. Rep. **5**, 10829 (2015).

[8] M. G. Rosenblum and A. S. Pikovsky, Phys. Rev. E **64**, 045202 (2001); M. G. Rosenblum, L. Cimponeriu, A. Bezerianos, A. Patzak, and R. Mrowka, *ibid.* **65**, 041909 (2002); B. Kralemann, L. Cimponeriu, M. Rosenblum, A. Pikovsky, and R. Mrowka, *ibid.* **76**, 055201 (2007); **77**, 066205 (2008).

[9] R. F. Galán, G. B. Ermentrout, and N. N. Urban, Phys. Rev. Lett. **94**, 158101 (2005).

[10] B. Kralemann, A. Pikovsky, and M. Rosenblum, Chaos **21**, 025104 (2011).

[11] I. H. Stevenson *et al.*, Curr. Opin. Neurobiol. **18**, 582 (2008); P. A. Valdes-Sosa *et al.*, NeuroImage **58**, 339 (2011).

[12] A. Pikovsky, M. Rosenblum, and J. Kurths, *Synchronization. A Universal Concept in Nonlinear Sciences* (Cambridge University Press, Cambridge, 2001).

[13] E. M. Izhikevich, *Dynamical Systems in Neuroscience* (MIT Press, Cambridge, MA, 2007).

[14] B. Kralemann, A. Pikovsky, and M. Rosenblum, New J. Phys. **16**, 085013 (2014).

[15] W. Penny, V. Litvak, L. Fuentemilla, E. Duzel, and K. Friston, J. Neurosci. Methods **183**, 19 (2009); C. Cadieu and K. Koepsell, Neural Comput. **22**, 3107 (2010).

[16] T. Stankovski, A. Duggento, P. V. E. McClintock, and A. Stefanovska, Phys. Rev. Lett. **109**, 024101 (2012); T. Rings and K. Lehnertz, Chaos: Interdisc. J. Nonlin. Sci. **26**, 093106 (2016).

[17] R. Mirollo and S. Strogatz, SIAM J. Appl. Math. **50**, 1645 (1990); U. Ernst, K. Pawelzik, and T. Geisel, Phys. Rev. Lett. **74**, 1570 (1995); C. van Vreeswijk, Phys. Rev. E **54**, 5522 (1996); W. Gerstner, Phys. Rev. Lett. **76**, 1755 (1996); P. Mohanty and A. Politi, J. Phys. A: Math. Gen. **39**, L415 (2006); V. A. Makarov, F. Panetsos, and O. de Feo, J. Neurosci. Methods **144**, 265 (2005).

[18] R.-M. Memmesheimer and M. Timme, Phys. Rev. Lett. **97**, 188101 (2006); W. Kinzel, J. Comput. Neurosci. **24**, 105 (2008); D. Patnaik, P. Sastry, and K. Unnikrishnan, Sci. Program. **16**, 49 (2008); O. Sporns, G. Tononi, and R. Kötter, PLoS Comput. Biol. **1**, e42 (2005); V. J. Barranca, D. Zhou, and D. Cai, Phys. Rev. E **93**, 060201 (2016).

[19] A. T. Winfree, *The Geometry of Biological Time* (Springer, Berlin, 1980); L. Glass and M. C. Mackey, *From Clocks to Chaos: The Rhythms of Life* (Princeton University Press, Princeton, NJ, 1988).

[20] C. C. Canavier, Scholarpedia **1**, 1332 (2006).

[21] D. Hansel, G. Mato, and C. Meunier, Neural Comput. **7**, 307 (1995).

[22] C. Morris and H. Lecar, Biophys. J. **35**, 193 (1981); J. Rinzel and B. Ermentrout, in *Methods of Neuronal Modeling*, edited by C. Koch and I. Segev (MIT Press, Cambridge, MA, 1998), pp. 251–292.

[23] A. Pikovsky, Phys. Rev. E **93**, 062313 (2016).

[24] When neither PRC nor ε_i are known, Eq. (3) represent a nonlinear system with respect to $N + 2N_F + 2$ unknowns. Alternatively, one could consider products of ε_i and the Fourier coefficients as unknowns and end up with a linear, but rather large system of $N(2N_F + 2)$ unknowns.

[25] Notice that error Δ_ε is minimized due to normalization according to Eq. (6).

[26] Parameters of the system Eqs. (10) and (11) are: $g_L = 0.5$, $g_K = 2$, $V_1 = -0.01$, $V_2 = 0.15$, $V_{Ca} = 1$, $V_K = -0.7$, $V_L = -0.5$, $g_{Ca} = 1.33$, $V_3 = 0.1$, $V_4 = 0.145$.